Received: 2 March 2018 | Revised: 25 June 2018 | Accepted: 3 July 2018

DOI: 10.1002/humu.23589

RESEARCH ARTICLE

WILEY HGVS HUMAN GENOME VARIATION SOCIETY

A mutation of *SCN1B* associated with GEFS+ causes functional and maturation defects of the voltage-dependent sodium channel

Debora Baroni | **Cristiana Picco** | **Oscar Moran**

Istituto di Biofisica, CNR, Genova, Italy

Correspondence
Debora Baroni, Istituto di Biofisica, CNR, Via De Marini, 6, 16149 Genova, Italy.
Email: dbaroni@ge.ibf.cnr.it

Funding information
This work was partially supported by Fondazione Compagnia di San Paolo.

Communicated by Garry R. Cutting

Abstract

Voltage-dependent sodium channels are responsible of the rising phase of the action potential in excitable cells. These integral membrane proteins are composed of a pore-forming α-subunit, and one or more auxiliary β subunits. Mutation p.Asp25Asn (D25N; c.73G > A) of the β1 subunit, coded by the gene *SCN1B*, has been reported in a patient with generalized epilepsy with febrile seizure plus type 1 (GEFS+). In human embryonic kidney 293 (HEK) cells, the heterologous coexpression of D25N-β1 subunit with Nav1.2, Nav1.4, and Nav1.5 α subunits, representative of brain, skeletal muscle, and heart voltage gated sodium channels, determines a reduced sodium channel functional expression and a negative shift of the activation and inactivation steady state curves. The D25N mutation of the β1 subunit causes a maturation (glycosylation) defect of the protein, leading to a reduced targeting to the plasma membrane. Also the β1-dependent gating properties of the sodium channels are abolished by the mutation, suggesting that D25N is no more able to interact with the α subunit. Our work underscores the role played by the β1 subunit, highlighting how a defective interaction between the sodium channel constituents could lead to a disabling pathological condition, and opens the possibility to design a mutation-specific GEFS+ treatment based on protein maturation.

KEYWORDS
epilepsy, GEFS+, protein maturation voltage-gated sodium channel

1 | INTRODUCTION

Action potential generation and propagation in excitable cells occur through, and are regulated by the function of voltage-gated sodium channels (NaCh), proteins with selective pores for sodium ions that span the cell membrane. In mammals, NaCh are heterotrimeric complexes composed of a pore-forming α-subunit (~260 kDa), and two of four ancillary subunits (β1-4, ~30–40 kDa; Catterall, 2012; Messner & Catterall, 1985). Nine different voltage-gated α subunits designated Nav1.1–Nav1.9 have been found in mammals, each encoded by a different gene, *SCN1A* to *SCN11A* (Catterall, Goldin, & Waxman, 2005). The polypeptides coded by these genes have a high degree of sequence identity, but a distinctive tissue specificity of gene expression (Catterall, 2012; Kruger & Isom, 2016).

All β subunits, encoded by genes *SCN1B* to *SCN4B*, contain an extracellular immunoglobulin (Ig)-loop motif present in the Ig superfamily of cell adhesion molecules (CAMs) (Isom & Catterall, 1996; Morgan et al., 2000; Yu et al., 2003). The highly conserved extracellular Ig motif is stabilized by an intrachain disulfide bridge (Barbieri, Baroni, & Moran, 2012; Isom & Catterall, 1996). The closely related β1 (MIM# 600235) and β3 (MIM# 608214) subunits (~45% sequence identity) are noncovalently associated with the α subunits, whereas the β2 (MIM# 601327) and the β4 (MIM# 608256) subunits (35% identity) are linked through a disulfide bond to the α subunits (Yu & Catterall, 2003). The β subunits modulate channel kinetics and voltage dependence (Ferrera & Moran, 2006; Isom, 2001; Moran, Conti, & Tammaro, 2003), regulate cell surface channel expression (Baroni, Barbieri, Picco, & Moran, 2013; Baroni & Moran, 2015a, 2015b; Baroni, Picco, Barbieri, & Moran, 2014), and contribute to cell–cell and cell–matrix adhesion, participating in cellular aggregation, ankyrin recruitment, and neurite outgrowth (Davis, Chen, & Isom, 2004; Malhotra, Kazen-Gillespie, Hortsch, & Isom, 2000; Malhotra et al., 2002; Ratcliffe, Westenbroek, Curtis, & Catterall, 2001). NaCh β subunits are all detectable in brain tissues, peripheral nerves, heart, and skeletal muscle (Catterall, 2012; Catterall et al., 2005; Yu & Catterall, 2003).

A number of inherited disorders have been associated with NaCh mutations, including skeletal muscle diseases, cardiac disorders, migraine, and epilepsy (Andavan & Lemmens-Gruber, 2011; George, 2005). Focusing on the β1 subunit, mutations in this subunit cause inherited diseases that selectively affect the central nervous system or

the heart, such as generalized epilepsy with febrile seizure plus type 1 (GEFS+) (MIM# 604233), the Dravet syndrome (MIM# 617350), the Brugada syndrome 5 (612838), and cardiac conduction diseases (MIM# 612838) (Baroni & Moran, 2015b). The substitution of aspartate for asparagine in position 25 (p.Asp25Asn, D25N; c.73G > A) in the β1 subunit has been correlated with GEFS+ (Orrico et al., 2009). This miss-sense mutation, found in a mutational analysis of patients with idiopathic childhood epilepsies, likely had occurred *de novo*, as it was absent in both parents (Orrico et al., 2009). Here, we studied the regulation of the expression of the NaCh subunit by WT- and D25N-β1 subunits. We have investigated the consequence of the β1 subunit mutation D25N on the channel formed by the isoform Nav1.2 (MIM#182390), as a paradigm of the central nervous system NaCh. Noteworthy, reports indicate that patients affected by GEFS+ usually do not manifest any cardiac or skeletal muscle symptoms, perhaps evidencing a selective interaction of this β1 mutation and the neuronal NaCh α subunit. Thus, we undertook the analysis of the D25N-β1 subunit effects also for Nav1.4 (MIM# 603967) and Nav1.5 (MIM# 600163), representative of skeletal muscle and cardiac voltage gated sodium α subunits, respectively. In all examined preparations, the effect of the D25N mutation of the β1 subunit on sodium current and α subunit protein expression resulted correlated with a NaCh intracellular traffic defect with the consequent failure of the mutated β1 subunit to modulate the voltage sensitivity of the channel. This finding offers a new target for the treatment of NaCh-related epilepsy based on a protein maturation management.

2 | MATERIAL AND METHODS

2.1 | Cell culture and transfection

Human embryonic kidney 293 (HEK) cells were grown in Ham's F10 medium supplemented with 2 mM L-glutamine and 10% fetal bovine serum (FBS), at 37°C and 5% CO_2. To prevent the loss of differentiation potential, cells were not allowed to become confluent. Experiments were done with three representative NaCh α subunit isoforms: Nav1.2 (NM_021007.2) that expresses preferentially in the brain (a gift from Fabrizia Cesca, Istituto Italiano di Tecnologia, Center for Synaptic Neuroscience, Genoa, Italy), the skeletal muscle isoform Nav1.4 (NM_000334.4) (a gift from Alfred L. George, Division of Genetic Medicine, Vanderbilt University School of Medicine, Nashville, TN), and the cardiac sodium channel Nav1.5 (NM_198056.2) (gift from Jean-Francois Desaphy, Università degli Studi di Bari, Department of Pharmacy & Drug Sciences, Bari, Italy). The plasmid construct containing the cDNA codifying for the human sodium channel ancillary β1 (NM_001037.4) subunit was a gift from Alfred L. George (Division of Genetic Medicine, Vanderbilt University School of Medicine, Nashville, TN). Mutant D25N of the β1 subunit was obtained using the QuickChange kit (Stratagene, Santa Clara, CA) according to the manufacturer's instructions. The mutation was verified by DNA sequencing (Biofab Research, Rome, Italy).

For transfection, HEK cells were plated onto poly-L-lysine-coated culture dishes and grown to 50% confluence in complete medium. Cells were transiently transfected using Lipofectamine 2000 (Invitrogen, Paisley, UK) with 2 μg of cDNA coding for a NaCh α subunit and 2 μg of β1 subunit cDNA, and used between 48 and 72 hr after transfection. Efficiency of transfections was evaluated by immunofluorescence.

For the electrophysiological measurements, cells were cotransfected with 50 ng of pcI-CD8 cDNA and the success of transfection was tested using CD8 antigen coated microspheres (Dynabeads Dynal, Invitrogen, Waltham, MA). Transient expression was tested electrophysiologically between 48 and 72 hr after transfection. Only cells that showed the expression of CD8 receptor by capturing the CD8-antigen covered microspheres were used for the electrophysiological experiments.

2.2 | Detection of sodium channels α and β1 subunits by immunofluorescence

Transiently transfected HEK cells were immunofluorescence stained in order to examine the expression efficiency of each single construct. Cells were fixed with 4% paraformaldehyde, subsequently washed three times with PBS and afterwards permeabilized in PBS, 0.3% Triton X-100, and 10% normal goat serum. Cells were incubated overnight with polyclonal rabbit anti-Nav1,2 (1:200, Millipore, Billerica, MA), anti-Nav1.4 (1:200, Abcam, Cambridge, UK), anti-Nav1.5 (1:200, Millipore), or goat anti-β1 (1:500; Santa Cruz Biotechnologies, Santa Cruz, CA) primary antibodies diluted in PBS and 10% normal goat serum. After primary antibody incubation, cells were incubated for 2 hr in goat anti-rabbit secondary antibody coupled to fluorescein isothiocyanate for the detection of the Nav1.2, Nav1.4, or Nav1.5, and in donkey anti-goat labeled with tetramethylrhodamine for the detection of the β1 subunit. Samples were washed three times with PBS after each antibody step. Micrographies were collected using a laser scanning spectral confocal microscope (TCS SP2-AOBS; Leica Microsystems, Heidelberg, Germany). Image analysis was performed using Leica and ImageJ (Schneider, Rasband, & Eliceiri, 2012) softwares. Analysis was performed observing >500 cells for each condition from at least three independent experiments.

2.3 | RNA isolation, reverse transcription, and real-time quantitative polymerase chain reaction

Total RNA was isolated using the RNeasy Mini kit (Qiagen, Hilden, Germany), and first-strand cDNA was synthesized from 2 μg of RNA using the RevertAid First Strand cDNA Synthesis Kit and random hexamers according to the manufacturer's instructions (Fermentas, Burlington, Canada). First-strand cDNA from transfected HEK cells was employed as the template in real-time polymerase chain reaction (PCR) amplifications using pairs of oligonucleotide primers specific for the human Nav1.2, Nav1.4, or Nav1.5 and β1 subunits and amplification conditions as described elsewhere (Baroni & Moran, 2011, 2015). Glyceraldehyde-3-phosphate-dehydrogenase (GAPDH) was used as a reference gene. Changes in cDNA amount were quantified by real-time PCR (CFX Connect Real-Time PCR Detection System instrument, Bio-Rad Laboratories, Hercules, CA) by using the comparative Ct method. Each sample was run in triplicate.

2.4 | Electrophysiological measurements

Sodium currents were measured with the patch clamp technique in the whole cell configuration using an Axopatch 200B amplifier (Axon Instruments, Foster City, CA, USA). Borosilicate glass micropipettes were fire polished yielding a resistance from 1.5 to 2.5 MΩ with the working solutions. The pipette was filled with (in millimole): 20 NaCl, 120 CsF, 2 ethylene glycol-bis(2-aminoethylether)-N,N,N′,N′-tetraacetic acid (EGTA), 4-(2-hydroxyethyl)-1-piperazineethanesulfonic acid (Hepes) buffer at pH 7.3. The external solution had the following composition (in millimole): 145 NaCl, 2.5 KCl, 1 $MgCl_2$, 2 $CaCl_2$, 10 glucose, 10 HEPES at pH 7.3. The output of the patch clamp amplifier was filtered by the low-pass 4-pole Bessel filter with a cut-off frequency of 10 kHz and sampled at 50 kHz. The cell was kept at a holding potential of −120 mV. Pulse stimulation and data acquisition used 16 bit D–A and A–D converters (NI PCI-6221, National Instruments, Austin, TX) controlled by a PC with a custom acquisition program (Gepulse, users.ge.ibf.cnr.it/pusch/programsmik.htm). The remaining linear responses after analogical compensation were digitally subtracted with a standard P/4 protocol. Access resistance was always less than 8 MΩ, and series-resistance was carefully compensated (between 80 and 95%). All measurements were done at room temperature (21 ± 1°C). For all three isoforms, the amplitude of the sodium current increased up to two- to threefold during the first 10 min of the experiment, and achieved a stable level after 15–20 min (Cummins & Sigworth, 1996; Cummins et al., 1993; Moran, Nizzari, & Conti, 1999; Tammaro, Conti, & Moran, 2002). Therefore, all measurements were done after 20 min from the beginning of the experiment. To evaluate the functional expression of NaCh, the peak amplitude of the maximal sodium current was normalized to cell capacitance in order to obtain the sodium current density. Electrophysiological data were analyzed using a custom procedures developed under IgorPro (Wavemetrics, Lake Oswego, OR, USA). The voltage dependence for the channel activation was evaluated by fitting the peak sodium current, I_{peak}, elicited by different test pulse potentials V, using the equation:

$$I_{peak}(V) = \Gamma \frac{1}{1 + \exp\left[\left(V - V_{1/2}\right)/S_a\right]} \left(V - V_{Na}\right), \quad (1)$$

where Γ is the maximum sodium conductance, $V_{1/2}$ is the half activation potential, S_a is the slope of the function, and V_{Na} is the sodium equilibrium potential (49.5 ± 1.2 mV). To determine the voltage dependence of the steady-state inactivation, the sodium current was elicited by a fixed-amplitude test pulse preceded by a conditioning 100 ms pulse. The test pulse peak current, I_{test}, was plotted against the prepulse potential, V_{pp}, and fitted with:

$$\frac{I_{test}}{I_{max}} = \frac{1}{1 + \exp\left[\left(V_{pp} - V_h\right)/S_h\right]}, \quad (2)$$

where I_{max} is the maximum current, V_h is the half inactivation potential and S_h is the voltage dependence of inactivation. The recovery from inactivation was determined with a double pulse protocol, with a 10 ms prepulse to −20 mV to evoke the maximal inactivation, followed by a variable recovery interval (0.5–40 ms) of a hyperpolarized potential of −120 mV. The inactivation-recovered channels were then measured by a test pulse of −10 mV. Time constants of recovery from inactivation were estimated by fitting peak current at test pulse against the recovery time interval to a single exponential function.

2.5 | Western blot

Cells were lysed in a buffer containing 62.5 mM trisaminomethane (TRIS), 2% sodium dodecyl sulfate (SDS), and a cocktail of protease inhibitors (1 mM 4-(2-aminoethyl) benzenesulfonyl fluoride hydrochloride—AEBSF, 0.8 μM aprotinin, 0.2 μM leupeptin, 40 μM bestatin, 15 μM pepstatin A, 14 μM E-64). Protein concentration was determined using the method of Lowry (Lowry, Rosebrough, Farr, & Randall, 1951) with bovine serum albumin as the standard. Equal amounts of proteins (40 μg) were subjected to SDS polyacrylamide gel electrophoresis. Separated proteins were transferred to PVDF membrane (Millipore) for 1 hr at 100 V. The blots were then incubated with polyclonal rabbit anti-Nav1.2 (1:200, Millipore), anti-Nav1.4 (1:200, Abcam), anti-Nav1.5 (1:200, Millipore), or anti-β1 (1:500, Abnova, Taipei city, Taiwan) as primary antibodies, and with horseradish peroxidase conjugated goat anti-rabbit antibody (1:2,000), as secondary antibody. Immunodetection was performed using Amersham ECL PLUS detection reagents (GE Healthcare, Marlborough, MA) and the images were captured by using Amersham Hyperfilm ECL (GE Healthcare). Developed films (Kodak, Rochester, NY) were scanned using a flatbed scanner with a resolution of 1,200 dpi. The intensity of the electrophoretic bands was quantified from digital images using ImageJ. In order to confirm the homogeneity of the loaded proteins, immunoblots were stripped by incubating them in a buffer containing 62.5 mM TRIS pH 6.8, 10% SDS, and 1% β-mercaptoethanol for 30 min at 55°C, and reprobed with a polyclonal anti-actin primary antibody (1:2,000, Sigma Aldrich). The intensity of each band was normalized to the intensity of the band corresponding to the actin detected in the stripped PVDF membranes.

2.6 | Deglycosylation assay

For deglycosylation experiments, protein deglycosylation Mix II (New England Biolabs, Ipswich, MA) was used according to the manufacturer's instructions with some modifications. Deglycosylation Mix Buffer 2 (10 μl) was added to total cell lysates from transiently transfected HEK cells. Samples were incubated at 75°C for 10 min. After cooling on ice, denatured proteins were supplemented with Protein Deglycosylation Mix II (10 μl) and incubated at room temperature for 30 min. Samples were finally incubated at 37°C for 3 hr. The extent of Nav1.2, Nav1.4, Nav1.5, and β1 deglycosylation was assessed by SDS-PAGE and Western blot analysis.

2.7 | Surface biotinylation

Transfected cell were grown in four T75 flasks; membrane proteins were biotinylated using the Pierce Cell Surface Protein Isolation Kit (Thermo Fisher Scientific, Waltham, MA) following the manufacturer's instructions. Briefly, intact cells were washed once with ice-cold PBS, resuspended at a concentration of 10^7 cells/mL in ice-cold

biotinylation mix (12 mg NHS-SS-biotin dissolved in 12 mL ice-cold PBS, pH 8.0), and incubated for 30 min at 4°C. Biotinylation of cell surface proteins was quenched by the addition of 1 mL quenching solution (Thermo Fisher Scientific). Labeled cells were washed twice in ice-cold TRIS-buffered saline, pH 7.4, and centrifuged at 500 × *g* for 3 min. The pellet was dispersed in 100 μL 50 mM TRIS-HCl, pH 7.6, using the plunger of a 1-mL syringe with a 36 gauge needle, and the preparation was made up to a final volume of 500 μL lysis buffer at a final concentration of 0.5% (w/v) SDS, 1% (v/v) Triton, 150 mM NaCl, 1 mM EDTA, 10 mM Tris-HCl, protease inhibitor cocktail, and 0.1 mg/mL phenylmethanesulfonyl fluoride (PMSF). Samples were ultrasonicated for 30 s at medium power (UP200Ht, Hielscher Ultrasonics, Teltow, Germany) at 4°C, and the lysates were centrifuged for 10 min at 16,000 × *g*. Biotinylated cell surface proteins were enriched using 500 μL Neutravidin agarose beads (Thermo Fisher Scientific) for 2 hr at 4°C. Beads were washed three times with lysis buffer, then twice with lysis buffer containing 500 mM NaCl, and then once with salt-free lysis buffer. Biotinylated cell surface proteins were eluted from beads by incubation for 1 hr at room temperature in 1% (w/v) SDS, 50 mM DTT, 100 mM Tris-HCl. Proteins were denatured subsequently by heating for 20 min at 50°C. Samples were loaded on SDS-PAGE gel and processed for Western blot. Quantified immunoreactive signals were normalized to cadherin, a cell surface housekeeping protein. In every experiment, biotinylated and cell lysate proteins from transiently transfected HEK samples were also probed with anti-GM130 primary antibody (1:200, BD Biosciences, San Josè, CA), which is a cis-Golgi marker (Nakamura et al., 1995).

2.8 | Statistics

All data are given as mean ± standard error of the mean (*SEM*). Statistical significance of differences among mean values was assessed by using the Kruskal–Wallis *H* test (one-way ANOVA on ranks). Differences were regarded as statistically significant for a probability, $P < 0.05$.

2.9 | Chemicals

Except when indicated, all reagents were purchased from Sigma-Aldrich (Milano, Italy).

3 | RESULTS

3.1 | Evaluation of transfection efficiency and mRNA abundance

We aimed to study the functional and biochemical effects of the mutated D25N-β1 subunit when heterologously coexpressed with three different NaCh pore-forming subunits, Nav1.2, Nav1.4, and Nav1.5, that are representative of brain, skeletal muscle, and heart channels, respectively. To this end, we first determined by immunofluorescence the transfection efficiency of vector constructs containing the cDNAs codifying for Nav1.2, Nav1.4, Nav1.5, WT-β1, or D25N-β1 NaCh subunits. As observable in Table 1, for each set of data (α, WT-β1, and D25N-β1 subunits), the transfection efficiency for either α and β1 subunits resulted not different; therefore, it was not necessary to proceed to any further correction of the results of mRNA and protein expression.

The same behavior was found for the relative abundance of each NaCh subunit mRNA, evaluated by real-time PCR (Table 1). The expression level of the mRNA coding for either α and β1 subunits resulted very similar for each α isoform. The mRNA coding for Nav1.2 resulted less abundant than that coding for Nav1.4 and Nav1.5, but no differences were found for preparations where Nav1.2 cDNA was transfected alone or cotransfected with WT- or D25N-β1. In untransfected HEK cells, neither NaCh subunits nor mRNA codifying for these subunits was detected.

3.2 | Functional expression of sodium channels in transfected HEK cells

The expression of Nav1.2, Nav1.4, and Nav1.5 alone or coexpressed with WT or D25Nβ1 resulted in typical voltage-gated sodium currents (Figure 1). Figure 1a shows traces of the brain isoform, Nav1.2, sodium currents evoked by 20 ms depolarizing pulses from a holding potential of −120 mV to a test potential from −70 to +60 mV in 5 mV increments. Coexpression of Nav1.2 and WT-β1 significantly increased ($H = 5.1$, $P = 0.025$) sodium current over Nav1.2 alone, while currents recorded with Nav1.2 coexpressed with D25N-β1 were not different from Nav1.2 alone ($H = 0.004$; $P = 0.935$). Figure 1b summarizes the mean current densities of Nav1.2 and Nav1.2 coexpressed with WT- and D25N-β1 subunits. A similar trend was observed in the other two α subunits investigated. Also with the skeletal muscle isoform, Nav1.4 (Figure 1c and d), and the cardiac channel, Nav1.5 (1e, f), the WT-β1 subunit significantly augments the sodium current density ($H = 5.66$, $P = 0.018$ and $H = 4.44$, $P = 0.038$ for Nav1.4 and Nav1.5, respectively), and the D25N mutant abolishes the β1 capacity to favor the sodium current density increase ($H = 0.30$, $P = 0.557$ and $H = 4.11$, $P = 0.704$ for Nav1.4 and Nav1.5, respectively). The values of peak sodium current density are shown in Table 2.

WT-β1 produced significant negative shifts ($P < 0.05$) in the voltage dependence of NaCh activation ($H = 5.44$, $P = 0.021$; $H = 5.35$, $P = 0.022$; and $H = 14.52$, $P < 0.001$ for Nav1.2, Nav1.4, and Nav1.5, respectively) and inactivation ($H = 10.4$, $P = 0.001$; $H = 6.83$, $P = 0.009$; and $H = 9.17$, $P = 0.002$ for Nav1.2, Nav1.4, and Nav1.5, respectively) when coexpressed with all three NaCh α isoforms, without modifying their slope (Table 3 and Figure 2). Differently, when each analyzed α subunit was cotransfected with D25N-β1, there was no shift of the activation ($H = 0.02$, $P = 0.626$; $H = 0.001$, $P = 0.951$; and $H = 0.07$, $P = 0.757$ for Nav1.2, Nav1.4, and Nav1.5, respectively) and inactivation ($H = 0.02$, $P = 0.860$; $H = 0.02$, $P = 0.860$; and $H = 001$, $P = 0.947$ for Nav1.2, Nav1.4, and Nav1.5, respectively) curves that resulted similar to those transfected with the sole α subunit (Figure 2). Coexpression of WT- or mutant β1 with the NaCh α subunit isoforms does not alter the recovery from inactivation at −120 mV (data not shown).

Our results demonstrate that mutation D25N inhibits the increment of functional expression of NaCh currents induced by the expression of the WT-β1 subunit, and abolishes the shift of the voltage

TABLE 1 Evaluation of transfection efficiency and mRNA abundance

	Nav1.2		Nav1.4		Nav1.5	
	α	$\beta1$	α	$\beta1$	α	$\beta1$
Percentage of transfected cells						
α	57.1 ± 4.4%	0	66.2 ± 4.0%	0	70.1 ± 3.3%	0
α+WT-β1	58.7 ± 9.8%	55.7 ± 2.8%	66.1 ± 3.3%	66.3 ± 8.4%	73.0 ± 2.6%	74.1 ± 7.2%
α+D25N-β1	56.0 ± 1.3%	59.1 ± 3.4%	64.3 ± 0.8%	65.0 ± 5.3	69.2 ± 4.0%	72.2 ± 2.6%
Normalized mRNA abundance						
α	0.44 ± 0.12	0	0.80 ± 0.02	0	0.80 ± 0.01	0
α+WT-β1	0.46 ± 0.10	0.80 ± 0.02	0.76 ± 0.05	0.78 ± 0.04	0.81 ± 0.04	0.77 ± 0.01
α+D25N-β1	0.40 ± 0.07	0.76 ± 0.05	0.78 ± 0.01	0.84 ± 0.03	0.84 ± 0.03	0.76 ± 0.01

The transfection efficiency was evaluated by immunocytochemistry from data obtained from at least three independent preparations, observing >500 cells for each condition. The mRNA abundance was obtained by real-time PCR and retrieved data were normalized to the expression of the housekeeping gene.

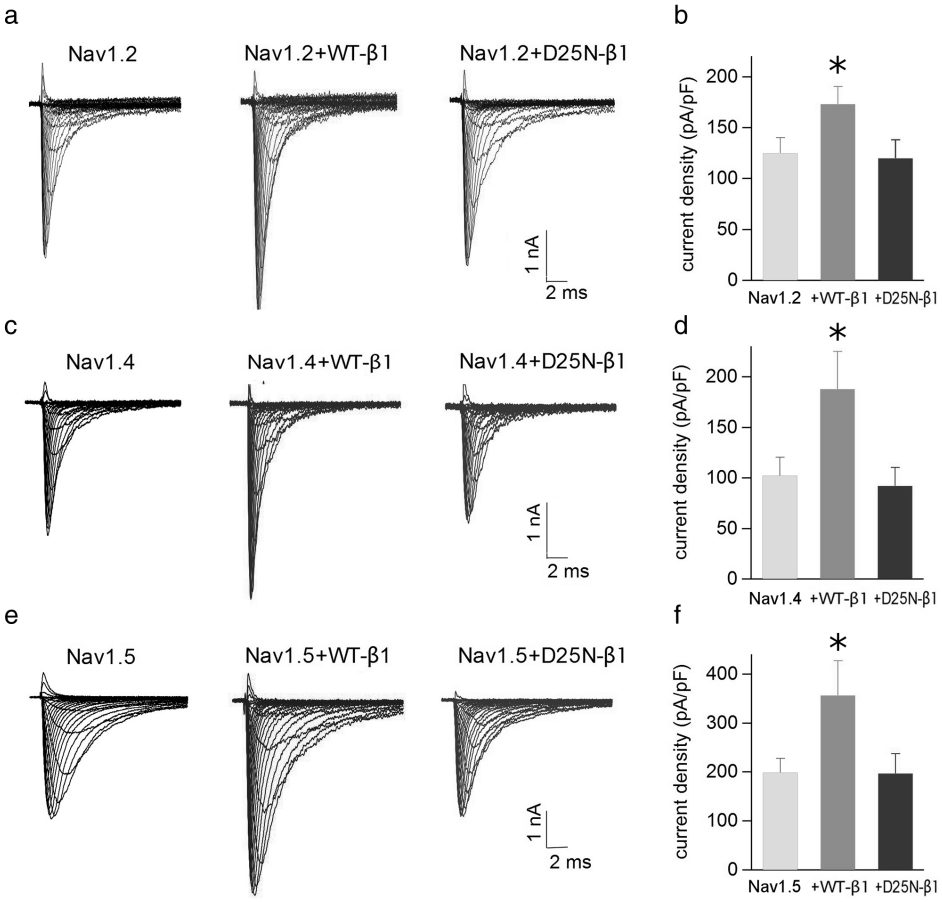

FIGURE 1 Functional expression of sodium channel Nav1.2, Nav1.4, and Nav1.5 in HEK cells. Comparison of families of whole cell currents elicited by depolarizations from −70 to +60 mV in HEK cells transfected with Nav1.2, Nav1.2 + WT-β1, and Nav1.2 + D25N-β1 (a), with Nav1.4, Nav1.4 + WT-β1, and Nav1.4 + D25N-β1 (c) and with Nav1.5, Nav1.5 + WT-β1, and Nav1.5 + D25N-β1 (e). The bars in (b), (d), and (f) represent the average (± *SEM*) of the peak current density evoked by a depolarizing pulse of −25 mV for Nav1.2, Nav1.4, and Nav1.5, respectively; the asterisk indicates statistically significant differences ($P < 0.05$) of data from Nav1.2, Nav1.4, and Nav1.5 transfected samples, respectively. The number of measurements is indicated in Table 2

dependence of activation and inactivation that is normally produced by the ancillary NaCh subunit.

3.3 | Expression of sodium channel proteins

Western blots of total lysates of HEK cells transfected with Nav1.2, Nav1.2 + WT-β1, and Nav1.2 + D25N-β1 reveal the expression of NaCh β1 and α subunits (Figure 3a). Images reveal either Nav1.2 and β1 subunits as two electrophoretic bands of slightly different molecular weights (grey and white head arrows in Figure 3a and b). Control experiments showed that antibodies against α or β1 subunits did not reveal the presence of these NaCh subunits in untransfected HEK cells. The same pattern of two electrophoretic bands was also observed in Western blots of total cell lysates of the Nav1.4 and

TABLE 2 Average sodium current density ± *SEM* (number of experiments) measured on HEK cells transfected with the sole α subunits, and cotransfected with the α plus the WT- and D25N-β1 subunits

	Current density (pA/pF)		
	Nav1.2	Nav1.4	Nav1.5
α	125 ± 15 (19)	87 ± 17 (14)	210 ± 27 (13)
α+WT-β1	173 ± 17 (11); $H = 5.10$, $P = 0.025^*$	188 ± 37 (10); $H = 5.35$, $P = 0.022^*$	356 ± 60 (16); $H = 4.44$, $P = 0.038^*$
α+D25N-β1	120 ± 18 (12); $H = 0.004$, $P = 0.935$	92 ± 18 (8); $H = 0.30$, $P = 0.557$	197 ± 40 (8); $H = 0.11$, $P = 0.704$

H is the Kruskal–Wallis test value and *P* is the probability of comparison with the corresponding α alone. The asterisk indicates a significant difference.

TABLE 3 The average of the activation and inactivation parameters ± *SEM* measured on HEK cells transfected with the sole α subunits, and co-transfected with the α plus the WT- and D25N-β1 subunits

	$V_{1/2}$ (mV)	S_a (mV)	n_a	V_h (mV)	S_h (mV)	n_h
Nav1.2	−23.4 ± 0.6	6.4 ± 0.2	(16)	−60.4 ± 1.0	6.4 ± 0.2	(16)
Nav1.2 + WT-β1	−25.3 ± 1.1	6.3 ± 0.2*	(9)	−65.9 ± 1.1*	6.4 ± 0.3	(11)
Nav1.2 + D25N-β1	−23.1 ± 0.6	6.5 ± 0.2	(11)	−60.7 ± 1.1	6.5 ± 0.2	(11)
Nav1.4	−23.0 ± 0.9	6.5 ± 0.4	(13)	−62.3 ± 1.4	6.0 ± 0.3	(11)
Nav1.4 + WT-β1	−26.0 ± 0.6	6.6 ± 0.3*	(10)	−67.8 ± 1.0*	6.1 ± 0.3	(10)
Nav1.4 + D25N-β1	−23.0 ± 0.8	6.6 ± 0.5	(9)	−61.6 ± 2.9	6.6 ± 0.4	(8)
Nav1.5	−36.8 ± 0.6	6.5 ± 0.3	(13)	−76.8 ± 1.6	8.1 ± 0.4	(12)
Nav1.5 + WT-β1	−43.2 ± 1.0	6.4 ± 0.4*	(16)	−86.0 ± 1.9*	8.3 ± 0.4	(13)
Nav1.5 + D25N-β1	−36.5 ± 2.3	6.7 ± 0.3	(8)	−77.3 ± 2.4	8.0 ± 0.3	(8)

$V_{1/2}$ is the half activation potential, S_a is the slope of the activation curve, V_h is the steady-state half inactivation potential, and S_h is the slope of inactivation curve. The number of experiments for activation (n_a) and inactivation (n_h) measurements is indicated in the brackets. The asterisk indicates a difference that is statistically different from data of sole α subunit.

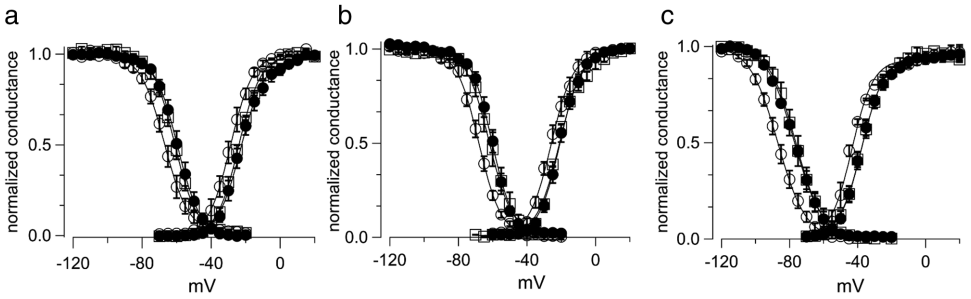

FIGURE 2 The voltage dependence of steady-state activation and inactivation curves of HEK cells expressing Nav1.2 (a), Nav1.4 (b), and Nav1.5 (c). Filled circles represent mean data from cells transfected with the sole α subunit, empty circles those cotransfected with WT-β1, and empty squares cells cotransfected with D25ND-β1. Bars are the *SEM*. Continuous lines represent the best fits of the activation curve with Eq. (1), and the inactivation curve with Eq. (2). Parameters of fitting and the number of experiments are reported in Table 3

Nav1.5 isoforms (Figure 3c–f). These bands may correspond to different glycosylation states of the NaCh subunits (Baroni, Picco, & Moran, 2017; Bennett, 2002). This hypothesis is confirmed, as removing both N- and O-linked glycans from both NaCh subunits, we obtained a single electrophoretic band, corresponding to the β1 and α unglycosylated proteins in cell transfected either with Nav1.2, Nav1.4, Nav1.5 alone or with WT- and D25N-β1 subunits (Figure 4a–c). Accordingly, the higher molecular weight bands were referred as corresponding to the fully glycosylated forms of β1 and α subunits of the NaCh, respectively. Instead, the lower molecular weight bands were considered as NaCh partially or unglycosylated forms. The quantification of total α and β1 subunit expression was done taking into account both bands. The total expression of β1 subunit protein in HEK lysates was very similar in cells transfected with Nav1.2 + WT-β1 and with Nav1.2 + D25N-β1 ($H = 0.310$, $P = 0.508$) (Figure 3a). However, the separate quantification of the fully glycosylated, and partially or unglycosylated forms of WT- and D25N-β1 yields very different outcome. The glycosylated fraction of the WT-β1 represents ~88% of the total protein, while this protein fraction is reduced to ~18% for the D25N-β1 (Figure 3a). The severe decrease of the glycosylated fraction of the mutant β1 protein is also observed when the ancillary subunit is expressed with the Nav1.4 and Nav1.5 isoforms (Figure 3c and e, respectively). When it is coexpressed with Nav1.4, the glycosylated fraction represents ~81% of the total WT-β1 subunit, but only ~14% of the total D25N-β1. Similarly, coexpression of Nav1.5 with WT-β1 or D25N results in a glycosylated fraction of ~70% and ~29%, respectively. We conclude that the mutation D25N impairs the glycosylation of the β1 subunit.

Important differences were found in the expression of Nav1.2 in total lysates when cells were cotransfected with WT-β1 and D25N-β1

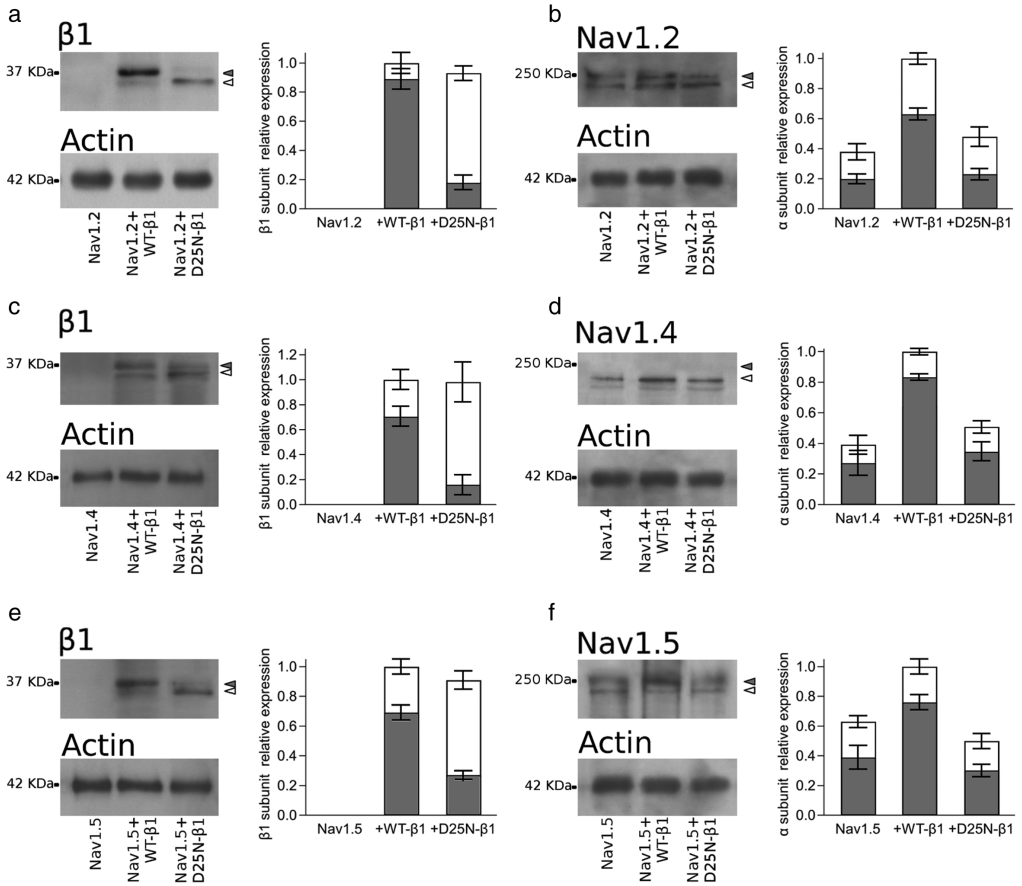

FIGURE 3 Expression of sodium channel β1, Nav1.2, Nav1.4, and Nav1.5 proteins in HEK cells. The Western blot images of the expression of β1 (at the top) and control actin bands (at the bottom) detected on the same blotting membrane expressed Nav1.2, Nav1.4, or Nav1.5 are shown in (a), (c), and (e), respectively, and those representing the expression of the sole α subunit (Nav1.2, Nav1.4, or Nav1.5) (at the top) and the corresponding control actin bands (at the bottom) are shown in (b), (d), and (f). In each image, the left lane corresponds to the total lysates of cells transfected with sole α subunit (Nav1.2, Nav1.4, or Nav1.5), the central lane to cells cotransfected with WT-β1, and the right lane to cells cotransfected with D25N-β1. In all cases, there are two bands one of a higher molecular weight, corresponding to the fully glycosylated, mature form, of the proteins (grey head arrows), and another of lower molecular weight, corresponding to the partially or unglycosylated, immature form, of the proteins (white head arrows). The relative expression of the protein is shown at the right of each panel. In each histogram, the lower part of each bar (grey) represents the glycosylated fraction, and the upper part of the bar represents the unglycosylated fraction of the protein. The bar high corresponds to the relative total protein expression. Data represent the mean and the standard error of the mean of data estimated from at least three independent experiments. The intensity of each band was scaled to the intensity of the band corresponding to the actin detected in the stripped blotting membrane, and successively was normalized to the average expression level of total β1 or total Nav1.2 in Nav1.2 +WT-β1 samples

(Figure 3b). Expression of the WT-β1 subunit determined an increase of 2.6-fold of total Nav1.2 protein expression, in comparison to Nav1.2 alone. Differently, cotransfection of the mutant D25N-β1 determined a significant lesser increase (1.2-fold) of the expression of total Nav1.2 protein, indicating that the mutation compromises the capacity of the β1 subunit to enhance the expression of the α subunit. This loss of α subunit expression enhancement is likewise observed in Nav1.4, where the α subunit expression increase of 3.4-fold by the WT-β1 is reduced to 1.1-fold by the β1 mutation (Figure 3d). Also expression enhancement of Nav1.5 by WT-β1 is reduced by the mutant, from 1.7- to 0.8-fold increase (Figure 3f). For all three α subunit isoforms, beside the increase of the total protein expression, the presence of WT-β1 modifies the glycosylation composition of the α protein, increasing the glycosylated fraction of the protein ($H = 8.33$, $P = 0.001$; $H = 8.34$, $P = 0.001$; and $H = 5.77$, $P = 0.017$ for Nav1.2, Nav1.4, and Nav1.5, respectively). Conversely, the D25N mutant keeps essentially unaltered the expression of the α subunit of either glycosylated ($H = 0.31$, $P = 0.519$; $H = 0.23$, $P = 0.565$; and $H = 0.53$, $P = 0.422$ for Nav1.2, Nav1.4, and Nav1.5, respectively) and partially or unglycosylated fractions, as it would be absent (Figure 3b, d, and f).

3.4 | Cell surface expression of sodium channels

The cell surface biotinylation experiments demonstrated that, compared to the WT-β1, the mutation D25N reduces the amount of the β1 subunit in the cell membrane (Figure 5). This observation, on the other hand, permits to affirm that the fully glycosylated fraction of the NaCh proteins is correlated with its presence in the plasma membrane. In order to ensure that the biotinylation reflects the specific labeling of proteins expressed on the cell surface, all immunoblots were also probed with anti-GM130 primary antibody, which specifically binds to a Golgi protein. As expected, no GM130

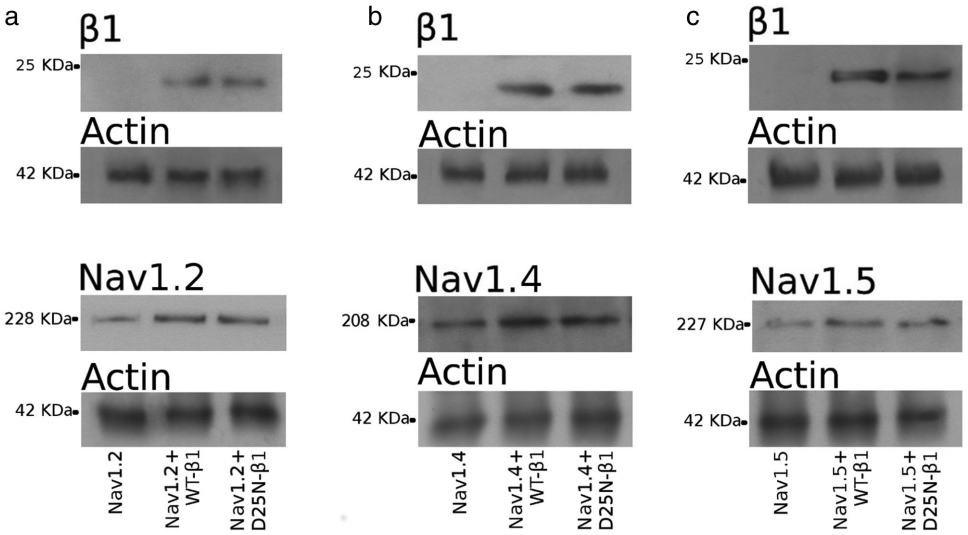

FIGURE 4 Treatment of the whole cell lysates with deglycosylation enzymes. Immunoblots revealing the $\beta 1$ subunit (upper panels) and the α subunit (lower panels) were obtained from extracts of cells transfected with Nav1.2 (a), Nav1.4 (b), and Nav1.5 (c). In each image, the left lane corresponds to the total lysates of cells transfected with the sole α, the central lane to cells transfected with α + WT-$\beta 1$, and the right lane to α + D25N-$\beta 1$. Digested NaCh protein samples are revealed as a unique immunoreactive band (at the top of each panel). Actin was used as housekeeping protein as control of loaded samples (at the bottom of each image)

signal was detected in NaCh biotinylated fractions compared to positive immunoblot detection observed in total lysate samples (Figure 5d).

Western blot quantification of the biotinylated α subunits shows that, compared with the sole α subunit, coexpression of WT-$\beta 1$ induced a significant increase of the α subunit expression on the cell surface ($H = 6.05$, $P = 0.009$; $H = 6.14$, $P = 0.008$; and $H = 7.76$, $P = 0.001$ for Nav1.2, Nav1.4 and Nav1.5, respectively) (Figure 6a–c). In contrast, the cell surface expression of Nav1.2, Nav1.4, and Nav1.5 was not significantly modified in cells cotransfected with D25N-$\beta 1$ ($H = 0.08$, $P = 0.632$; $H = 0.34$, $P = 0.473$; and $H = 0.1$, $P = 0.653$ for Nav1.2, Nav1.4 and Nav1.5, respectively; Figure 6a–c).

The biochemical analysis was confirmed by the direct localization of the NaCh α and $\beta 1$ subunits by immunofluorescence microscopy (Figure 7). Co-expression of WT-$\beta 1$ with Nav1.2, Nav1.4, and Nav1.5 (Figure 7a, c, and e, respectively) shows that the two NaCh subunits are strongly expressed in HEK-transfected cells. The merged images reveal the α and WT-$\beta 1$ subunits are colocalized in the cells, suggesting an interaction between these two proteins. Differently, when Nav1.2, Nav1.4, and Nav1.5 α subunits are expressed with the mutant D25N-$\beta 1$ (Figure 7b, d, and f, respectively), the two subunits are clearly segregated. The D25N-$\beta 1$ is mostly localized near to the center of the cells, while the α subunits are preferentially distributed in the cell periphery, resulting on an absence of colocalization of the two subunits, as revealed by the merged images.

4 | DISCUSSION

The mutation D25N of the NaCh $\beta 1$ subunit has been described in a patient with the clinical manifestations of the generalized epilepsy with febrile seizures plus-1 (MIM# 604233). However, the absence of the mutation in both parents has led to the conclusion that it is a *de novo* mutation (Orrico et al., 2009). We have characterized, for the first time, the biochemical and functional consequences of this mutation on the sodium channel function. We explored the protein expression of each NaCh subunit in cells transfected with α subunit alone, α subunit +WT-$\beta 1$, and α subunit +D25N-$\beta 1$. The presence of the RNA transcripts of every NaCh subunit was controlled in each preparation (Table 1). The relative concentrations of the RNA transcripts of WT- and D25N-$\beta 1$ subunits were comparable independently to the α subunit transfected. Also the abundance of the RNA transcripts of Nav1.4 and Nav1.5 were very similar, independently to the presence of the $\beta 1$ subunit, or the $\beta 1$ subunit isoform cotransfected. Instead, the concentration of the RNA transcript of Nav1.2 was lower than other NaCh species, but it was not influenced by the expression of the $\beta 1$ subunit (see Table 1). Thus, any functional alteration, or difference in the NaCh expression caused by the D25N mutation of the $\beta 1$ subunit described below could be considered as a posttranscriptional phenomenon. The most striking effect of the heterologous coexpression of the WT-$\beta 1$ subunit with the pore-forming α subunit is the augment of the expression of the NaCh, resulting in an increase of sodium current density (Aman et al., 2009; Baroni et al., 2017; Hanlon & Wallace, 2002; McCormick, Srinivasan, White, Scheuer, & Catterall, 1999; Meadows, Chen, Powell, Clare, & Ragsdale, 2002; Moran & Conti, 2001; Moran et al., 2003; Tammaro et al., 2002). The role of the ancillary $\beta 1$ subunit on the intracellular trafficking of the NaCh has been previously highlighted either in over-expression (Baroni & Moran, 2015; Baroni et al., 2013, 2017) or silencing experiments (Baroni et al., 2014). On the contrary, our results show how cotransfection of a NaCh α subunit with the mutant D25N-$\beta 1$ yields a sodium current level similar to that of cells transfected with an α subunit alone, either for the brain NaCh Nav1.2 (Figure 1b), the skeletal muscle isoform Nav1.4 (Figure 1d), and the cardiac channel Nav1.5 (Figure 1f). Thus, we explored the protein expression of each NaCh subunit. When we

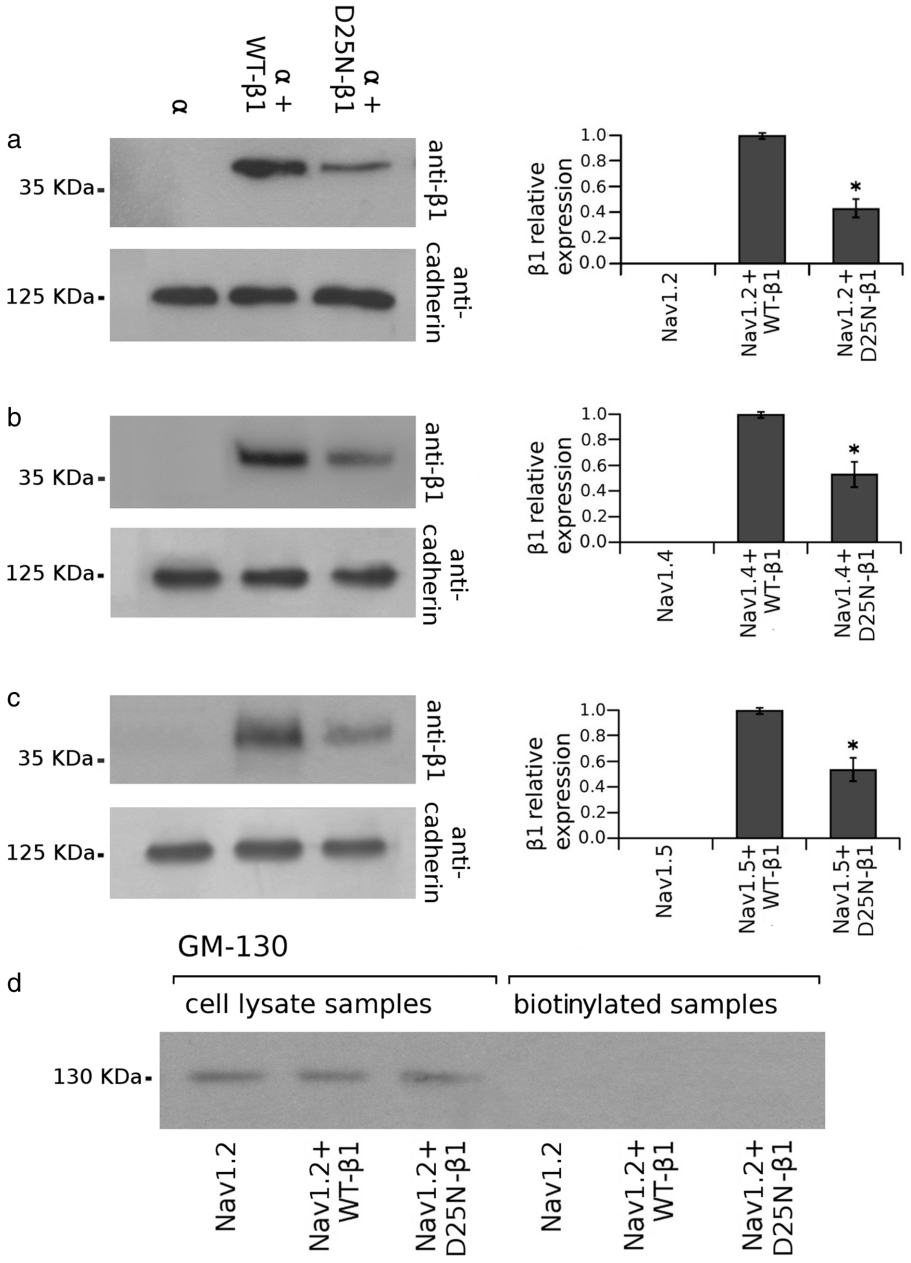

FIGURE 5 Cell surface expression of sodium channel β1 proteins in HEK cells. Western blots of the biotinylated fractions of WT-β1 and D25N-β1 co-transfected with Nav1.2 (a), Nav1.4 (b), and Nav1.5 (c). The plasma membrane marker cadherin, revealed on the same blotting membranes, has been used as control. Bar graphic at right of each Western blot set, showing the relative expression of β1 subunits, represents the mean and the *SEM* of data calculated from at least three independent experiments for each condition. The intensity of each band was scaled to the intensity of the band corresponding to the cadherin detected in the stripped blotting membrane and was normalized to the average expression level of total WT-β1 samples. (d) Anti-GM130 primary antibody was used as negative control to show that biotinylation revealed the specific labeling of only those NaCh proteins expressed on the cell membrane

evaluated the expression of NaCh proteins in transfected cells, both α and β1 proteins were detected in cell lysates as two electrophoretic bands of slightly different molecular mass. These double bands were observed in both WT- and D25N-β1, independently from the α subunit transfected isoform (Figure 3a, c, and e). Likewise, the double electrophoretic bands were present in the total lysates of cells transfected with Nav1.2 (Figure 3b), Nav1.4 (Figure 3d), and Nav1.5 (Figure 3f). These two different electrophoretic bands should correspond to distinct posttranslational glycosylation conditions, reflecting different maturation states of the NaCh proteins. Notice that glycosylation of membrane proteins is important for protein folding and stability and is essential for the intracellular trafficking and membrane localization of the channel (Lisowska & Jaskiewicz, 2001). To confirm this interpretation, we deglycosylated the proteins of total cell lysates with an enzymatic cocktail. This treatment resulted in a single band, roughly corresponding to the lower molecular weight band for each protein (Figure 4). Thus, the first band, of lower molecular mass, may correspond to an immature protein with few or no posttranslational

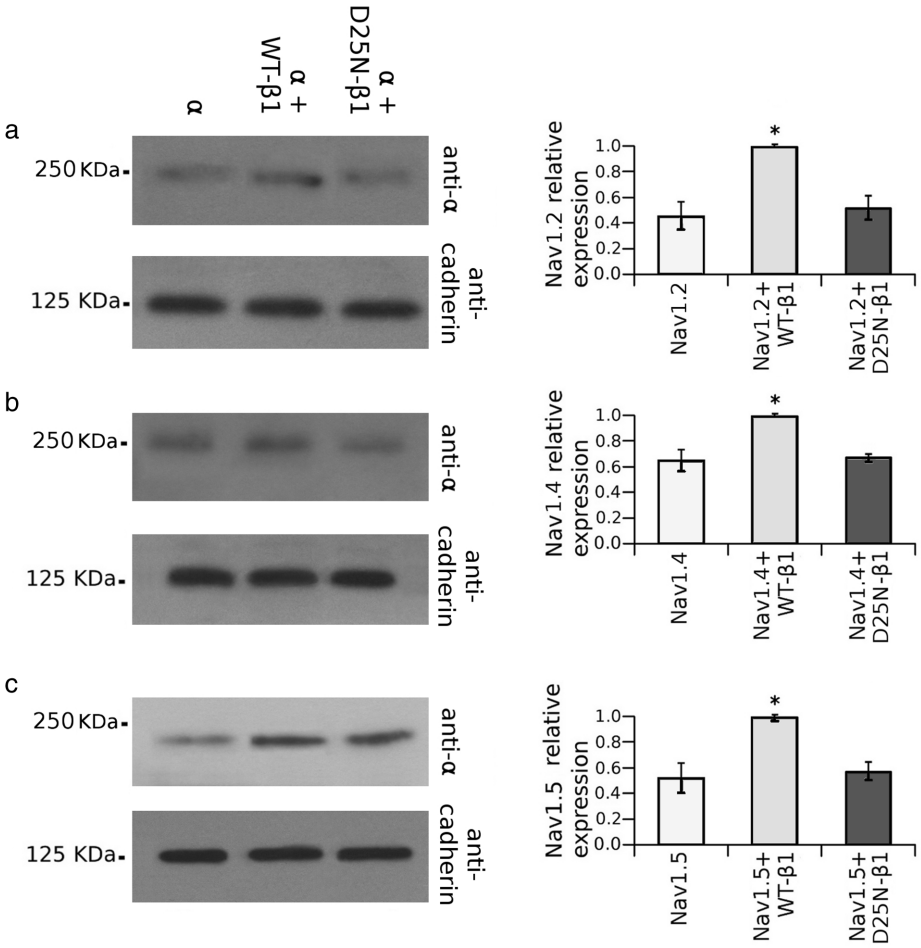

FIGURE 6 Cell surface expression of sodium channel α proteins in HEK cells. Western blots of the biotinylated fractions of Nav1.2 (a), Nav1.4 (b), and Nav1.5 (c) transfected in cells alone, or cotransfected with WT-β1, or D25N-β1. The plasma membrane marker cadherin, revealed on the same blotting membranes, has been used as control. Western blot set, showing the relative expression of α subunits, represents the mean ± *SEM* of data calculated from, at least three independent experiments for each condition. The intensity of each band was scaled to the intensity of the band corresponding to the cadherin detected in the stripped blotting membrane and was normalized to the average expression level of the α subunit coexpressed with WT-β1.

modifications. This fraction of protein, that is unglycosylated or only partially glycosylated, is probably waiting to be processed. Instead, the second band, of a higher molecular mass, should correspond to the mature polypeptide that has completely undergone the process of glycosylation (Baroni et al., 2017; Bennett, 2002; Bennett, Urcan, Tinkle, Koszowski, & Levinson, 1997; Mercier et al., 2015; Thornhill & Levinson, 1987). This fully glycosylated protein would be going to be trafficked to the plasma membrane or would be already reached it.

The relative abundance of the total WT- and D25N-β1 proteins—sum of the partially glycosylated (immature) and fully glycosylated (mature) fractions—is not statistically different, when they are coexpressed either with Nav1.2 (Figure 3a), Nav1.4 (Figure 3c), or with Nav1.5 (Figure 3e). What is strikingly are the differences in the relative amounts of immature and mature fractions of the WT- and D25N-β1 proteins. In all three conditions, the expression of the mature WT-β1 is significantly higher than that of the immature fraction. Contrary, the immature D25N-β1 is significantly more abundant than the mature fraction of the mutant protein. In principle, our quantification of the expression level of WT and D25N β1 subunit proteins let us argue that after being translated, the destiny of the WT and mutant β1 subunits is different. WT-β1 subunit completely completes its maturation process, being fully glycosylated and thereafter trafficked to the plasma membrane; conversely, mutant D25N arrests its maturation process, remaining trapped in the intracellular compartments as an uncompletely glycosylated protein. The high level of the immature, unglycosylated, D25N that is detected in the whole cell extracts further suggests that mutant β1 defects do not correlated with its folding as it is not processed for degradation by the proteasome. The larger abundance of the fully glycosylated, mature fraction, of the WT-β1 appears to be correlated with a higher expression of total Nav1.2 (Figure 3b), Nav1.4 (Figure 3d), and Nav1.5 (Figure 3f). In fact, in absence of the β1 subunit, the relative expression of the three subtypes of α subunit is low, as also occurs when the α subunits are expressed with the mutant D25N-β1, with a low abundance of the mature fraction.

We determined the abundance of the NaCh proteins in the plasma membrane with the biotinylation procedure. These experiments confirmed that WT-β1 subunit is more abundant in the membrane than the mutant D25N-β1 (Figure 5). Transfection of cells with the sole

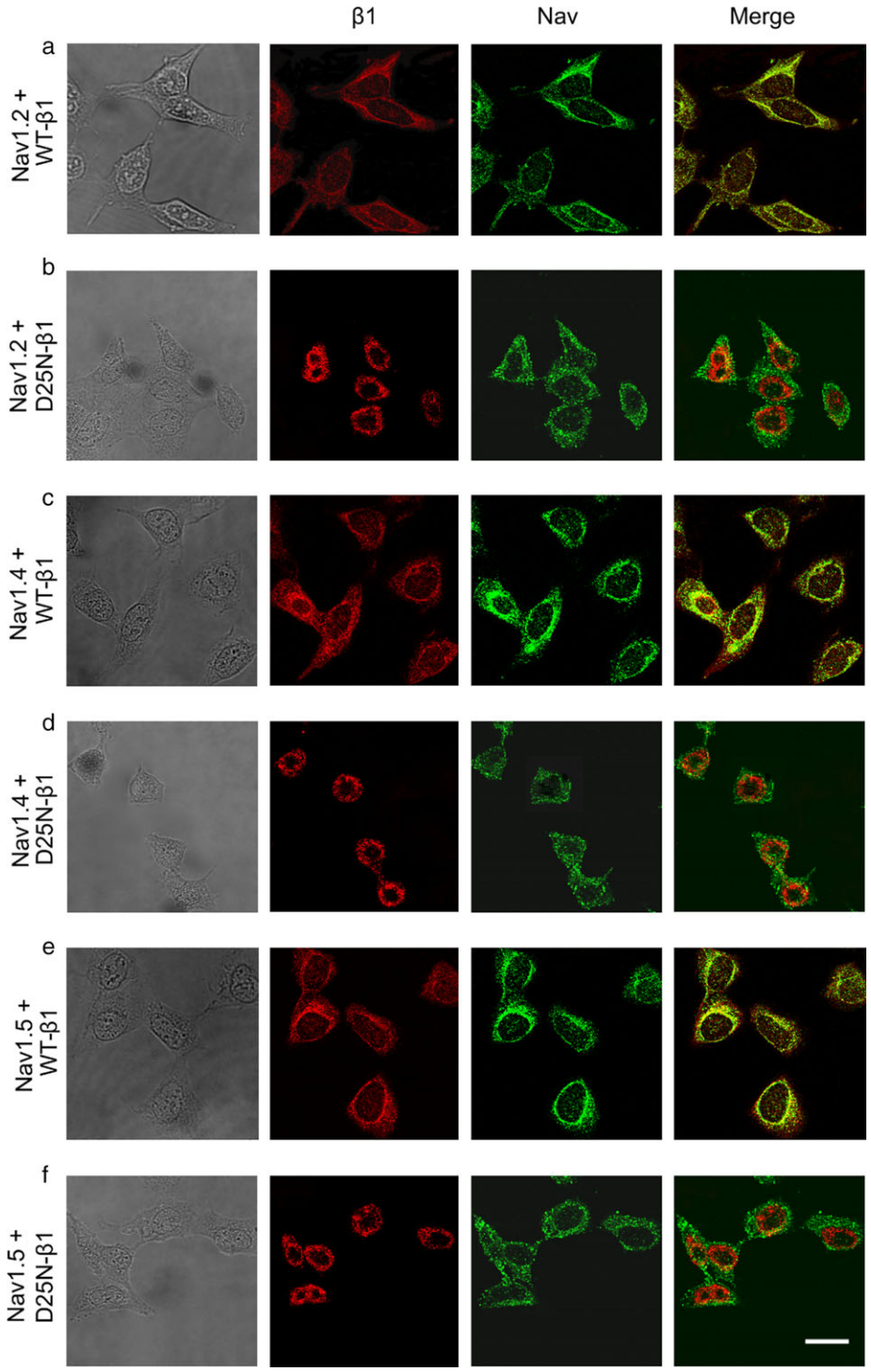

FIGURE 7 Cellular localization of NaCh α and β1 subunits. Microscopy images showing cells cotransfected with Nav1.2 +WT-β1 (a), Nav1.2 +D25N-β1 (b), Nav1.4 +WT-β1 (c), Nav1.4 +D25N-β1 (d), and Nav1.5 +WT-β1 (e), Nav1.5 +D25N-β1 (f). The first column shows the bright field images, and the second and third columns are the immunofluorescence images of the β1 subunit (red) and α subunit (green), respectively. The last column shows the merged images, displaying the α and β1 NaCh subunits colocalization in yellow. The scale bar is 15 μm.

α subunit yields a protein that is docked to the plasma membrane, but the abundance of α subunit protein is significantly enhanced by the presence of the WT-β1 (Figure 6). The lower abundance of the D25N-β1 subunit in the membrane seems to condition also the reaching of the α subunit to the plasma membrane (Figure 6). There are evidences that residues located both at the N- and C-termini ends of the β1 subunit are involved in noncovalent association with α subunits (McCormick et al., 1998, 1999; Meadows, Malhotra, Stetzer, Isom, & Ragsdale, 2001; Spampanato, Aradi, Soltesz, & Goldin, 2004). In particular, in the N-terminus of the protein, there are charged residues (E4, D6, and E8) that may serve as a scaffold for the noncovalent interaction with the pore-forming α subunit. The substitution of a negative charged residue (D) with a noncharged one (N) in position 25 of the polypeptide, which is a residue localized in the Ig loop in the

neighborhood of these critical residues, may prevent or weaken the capability of the β1 subunit to interact with its counterpart. Hence, mutation D25N, that impedes the correct maturation of the β1, results on an impairment of its association with the pore-forming α subunit, limiting its maturation and intracellular traffic to the cell membrane. The α-β1 subunits interaction was confirmed by the immunofluorescence experiments. The WT-β1 subunit is appreciably colocalized with Nav1.2 (Figure 7a), Nav1.4 (Figure 7c), and Nav1.5 (Figure 7e). This colocalization is dramatically belittled in cells coexpressing the α subunits and the mutant and D25N-β1 (Figure 7b, d, and f), confirming that the D25N mutation may reduce the β1 capability to interact with the α subunits. Interestingly, the WT-β1 induces a negative shift of the NaCh steady-state activation and inactivation curves (Baroni et al., 2017; Ferrera & Moran, 2006; Meadows et al., 2002). This shift is lost by the D25N-β1 (Figure 2 and Table 3), favoring the hypothesis of a α-mutant β1 interaction failure. Therefore, we propose that mutation D25N of the ancillary subunit may reduce the capability of the β1 to associate with the α subunit and drive the expression of the NaCh complex into the plasma membrane (Calhoun & Isom, 2014; Patino & Isom, 2010). In the presence of this β1 mutation, the availability of NaChs on the cell surface results reduced, and the shift of the voltage-dependence of the NaCh would lead to the destabilization of excitable cells. Even if the heterologous expression system could may not accurately reflect the in vivo situation, on the basis of our results, we could speculate that, as other epileptic intracellular trafficking defective mutations (Aman et al., 2009; Meadows et al., 2002; Patino et al., 2009; Tammaro et al., 2002; Xu et al., 2007), the presence of the D25N mutation in the β1 subunit would result in a larger population of sodium channels that are available to open at or near the resting membrane potential, a feature that may promote repetitive firing and lead to hyperexcitability.

An awkward question remains still open: although the β1 subunit is ubiquitously expressed, mutation affecting this NaCh subunit are selectively associated with CNS or heart pathologies (Baroni & Moran, 2015). However, mutation D25N of β1, that was described to produce a clinical profile of GEFS+, without association with cardiac or skeletal muscle diseases, actually also affects the NaCh α subunits representative of heart and muscle. We could hypothesize that in their natural environment, sodium channels are not regulated only by the β1 subunit, but also by the other ancillary subunits β2, β3 and β4 as well as by other NaCh comples interacting proteins that may have a role in the modulation of the intracellular traffic and function of the channel. In this context, a mutation that produces a defect in a β subunit could be compensated, or not, according to the NaCh pathway regulatory proteins expressed in different organs. Moreover, evidences indicate that the β1 subunit itself could have a role in the gene expression pattern of different cell types (Baroni & Moran, 2015; Baroni et al., 2013, 2014). In any case, to describe the pathogenesis of a central nervous system disease, it is necessary to consider also the interactions between β1 subunit and the proteins of the extracellular matrix that also influence the neurite growing (Davis et al., 2004; Kazarinova-Noyes et al., 2001; Malhotra et al., 2000, 2002; Ratcliffe et al. 2001).

In summary, our results show that the role of β1 subunit on the maturation and expression of the entire NaCh complex is of paramount importance to understand the pathological conditions resulted from a defective interaction between the NaCh constituents. The present study describes for the first time how the defects caused by mutation D25N of β1 subunit, produce modifications of NaCh activation properties as well as a reduction of the expression of the NaCh on the plasma membrane. This is congruent with a maturation defect of the mutant β1 subunit that fails its capacity to associate with the pore-forming α subunit and favor its translocation toward the plasma membrane. The behavior of D25N-β1 subunit includes this mutant subunit to the group of proteins related to diseases characterized by trafficking defects, as cystic fibrosis (MIM# 219700), Fabry disease (MIM# 301500), Gaucher disease (MIM# 230800), and Tay-Sachs disease (MIM# 272800), nephrogenic diabetes insipidus (MIM# 602024), oculocutaneous albinism (MIM# 203200), protein C deficiency (MIM# 278000), and many others (Sampson, Thomas, & Begley, 2007). This characteristic suggests the possibility to implement pharmacological strategies to rescue the mutant protein. One possibility could be the use of modulatory proteins such as β-subunits, calmodulin, or G protein $\beta 2\gamma 3$ whose administration has been proposed by Rusconi and coworkers (Rusconi et al., 2007, 2009) to correct the expression of a trafficking defective Nav1.1 (MIM# 182389) loss-of-function mutation (p.Met1841Thr). Analogously to what is today under investigation for the treatment of cystic fibrosis, Tay Sacks disease and Fabri disease, another possible pharmacological approach could be the development of correctors acting by improving the intracellular processing and the delivery of mutant β1 subunit to the plasma membrane and therefore attenuate the symptoms of the GEFS+ disease.

ACKNOWLEDGMENTS

This work was partially supported by Fondazione Compagnia di San Paolo. We thank Dr. Michael Pusch for comments and corrections.

ORCID

Debora Baroni http://orcid.org/0000-0001-8764-2468

REFERENCES

Aman, T. K., Grieco-Calub, T. M., Chen, C., Rusconi, R., Slat, E. A., Isom, L. L., & Raman, I. M. (2009). Regulation of persistent Na current by interactions between beta subunits of voltage-gated Na channels. *Journal of Neuroscience*, *29*, 2027–2042.

Andavan, G. S. B., & Lemmens-Gruber, R. (2011). Voltage-gated sodium channels: Mutations, channelopathies and targets. *Current Medicinal Chemistry*, *18*, 377–397.

Barbieri, R., Baroni, D., & Moran, O. (2012). Identification of an intramolecular disulfide bond in the sodium channel beta1-subunit. *Biochemical and Biophysical Research Communications*, *420*, 364–367.

Baroni, D., & Moran, O. (2011). Molecular differential expression of voltage-gated sodium channel α and β subunit mRNAs in five different mammalian cell lines. *Journal of Bioenergetics and Biomembranes*, *43*, 729–738.

Baroni, D., Barbieri, R., Picco, C., & Moran, O. (2013). Functional modulation of voltage-dependent sodium channel expression by wild type and mutated C121W-β1 subunit. *Journal of Bioenergetics and Biomembranes*, *45*, 353–368.

Baroni, D., & Moran, O. (2015a). Differential gene expression profiles of two excitable rat cell lines after over-expression of WT- and C121W-beta1 sodium channel subunits. *Neuroscience*, *297*, 105–117.

Baroni, D., & Moran, O. (2015b). On the multiple roles of the voltage gated sodium channel β1 subunit in genetic diseases. *Frontiers in Pharmacology*, *18*, 105–117.

Baroni, D., Picco, C., Barbieri, R., & Moran, O. (2014). Antisense-mediated post-transcriptional silencing of SCN1B gene modulates sodium channel functional expression. *Biologie Cellulaire*, *106*, 13–29.

Baroni, D., Picco, C., & Moran, O. (2017). Mutation E87Q of the β1-subunit impairs the maturation of the cardiac voltage-dependent sodium channel. *Scientific Reports*, *7*. Retrieved from https://www.nature.com/articles/s41598-017-10645-y

Bennett, E., Urcan, M. S., Tinkle, S. S., Koszowski, A. G., & Levinson, S. R. (1997). Contribution of sialic acid to the voltage dependence of sodium channel gating. A possible electrostatic mechanism. *Journal of General Physiology*, *109*, 327–343.

Bennett, E. S. (2002). Isoform-specific effects of sialic acid on voltage-dependent Na+ channel gating: Functional sialic acids are localized to the S5-S6 loop of domain I. *Journal of Physiology*, *538*, 675–690.

Calhoun, J. D., & Isom, L. L. (2014). The role of non-pore-forming β subunits in physiology and pathophysiology of voltage-gated sodium channels. *Handbook of Experimental Pharmacology*, *221*, 51–89.

Catterall, W. A., Goldin, A. L., & Waxman, S. G. (2005). International union of pharmacology. XLVII. Nomenclature and structure-function relationships of voltage-gated sodium channels. *Pharmacological Reviews*, *57*, 397–409.

Catterall, W. A. (2012). Voltage-gated sodium channels at 60: Structure, function and pathophysiology. *Journal of Physiology*, *590*, 2577–2589.

Cummins, T., & Sigworth, F. (1996). Impaired slow inactivation in mutant sodium channels. *Biophysical Journal*, *71*, 227–236.

Cummins, T., Zhou, Y., Sigworth, F., Ukomadu, C., Stephan, M., Ptácek, L. J., & Agnew, W. S. (1993). Functional consequences of a Na^+ channel mutation causing hyperkalemic periodic paralysis. *Neuron*, *10*, 667–678.

Davis, T. H., Chen, C., & Isom, L. L. (2004). Sodium channel beta1 subunits promote neurite outgrowth in cerebellar granule neurons. *Journal of Biological Chemistry*, *279*, 51424–51432.

Ferrera, L., & Moran, O. (2006). Beta1-subunit modulates the Nav1.4 sodium channel by changing the surface charge. *Experimental Brain Research Experimentelle Hirnforschung Experimentation Cerebrale*, *172*, 139–150.

George, A. L. J. (2005). Inherited disorders of voltage-gated sodium channels. *Journal of Clinical Investigation*, *115*, 1990–1999.

Hanlon, M. R., & Wallace, B. A. (2002). Structure and function of voltage-dependent ion channel regulatory beta subunits. *Biochemistry*, *41*, 2886–2894.

Isom, L., & Catterall, W. (1996). Na+ channel subunits and Ig domains. *Nature*, *383*, 307–308.

Isom, L. L. (2001). Sodium channel beta subunits: Anything but auxiliary. *Neuroscientist*, *7*, 42–54.

Kazarinova-Noyes, K., Malhotra, J. D., McEwen, D. P., Mattei, L. N., Berglund, E. O., Ranscht, B., … Xiao, Z. C. (2001). Contactin associates with Na+ channels and increases their functional expression. *Journal of Neuroscience*, *21*, 7517–7525.

Kruger, L. C., & Isom, L. L. (2016). Voltage-gated Na+ channels: Not just for conduction. *Cold Spring Harbor Perspectives in Biology*. https://doi.org/10.1101/cshperspect.a029264

Lisowska, E., & Jaskiewicz, E. (2001) Protein glycosylation, an overview. *ELS*. https://doi.org/10.1002/9780470015902.a0006211.pub3

Lowry, O. H., Rosebrough, N. J., Farr, A. L., & Randall, R. J. (1951). Protein measurement with the Folin phenol reagent. *Journal of Biological Chemistry*, *193*, 265–275.

Malhotra, J. D., Kazen-Gillespie, K., Hortsch, M., & Isom, L. L. (2000). Sodium channel beta subunits mediate homophilic cell adhesion and recruit ankyrin to points of cell-cell contact. *Journal of Biological Chemistry*, *275*, 11383–11388.

Malhotra, J. D., Koopmann, M. C., Kazen-Gillespie, K. A., Fettman, N., Hortsch, M., & Isom, L. L. (2002). Structural requirements for interaction of sodium channel beta 1 subunits with ankyrin. *Journal of Biological Chemistry*, *277*, 26681–26688.

McCormick, K., Isom, L., Ragsdale, D., Smith, D., Scheuer, T., & Catterall, W. A. (1998). Molecular determinants of the Na^+ channel function in the extracellular domain of the b1 subunit. *Journal of Biological Chemistry*, *273*, 3954–3962.

McCormick, K. A., Srinivasan, J., White, K., Scheuer, T., & Catterall, W. A. (1999). The extracellular domain of the beta1 subunit is both necessary and sufficient for beta1-like modulation of sodium channel gating. *Journal of Biological Chemistry*, *274*, 32638–32646.

Meadows, L., Malhotra, J. D., Stetzer, A., Isom, L. L., & Ragsdale, D. S. (2001). The intracellular segment of the sodium channel beta 1 subunit is required for its efficient association with the channel alpha subunit. *Journal of Neurochemistry*, *76*, 1871–1878.

Meadows, L. S., Chen, Y. H., Powell, A. J., Clare, J. J., & Ragsdale, D. S. (2002). Functional modulation of human brain Nav1.3 sodium channels, expressed in mammalian cells, by auxiliary beta 1, beta 2 and beta 3 subunits. *Neuroscience*, *114*, 745–753.

Mercier, A., Clément, R., Harnois, T., Bourmeyster, N., Bois, P., & Chatelier, A. (2015). Nav1.5 channels can reach the plasma membrane through distinct N-glycosylation states. *Biochimica et Biophysica Acta*, *1850*, 1215–1223.

Messner, D., & Catterall, W. (1985). The sodium channel from rat brain. Separation and characterisation of subunits. *Journal of Biological Chemistry*, *260*, 10597–10604.

Moran, O., & Conti, F. (2001). Skeletal muscle sodium channel is affected by an epileptogenic beta1 subunit mutation. *Biochemical and Biophysical Research Communications*, *282*, 55–59.

Moran, O., Conti, F., & Tammaro, P. (2003). Sodium channel heterologous expression in mammalian cells and the role of the endogenous beta1-subunits. *Neuroscience Letters*, *336*, 175–179.

Moran, O., Nizzari, M., & Conti, F. (1999). Myopathic mutations affect differently the inactivation of the two gating modes of sodium channels. *Journal of Bioenergetics and Biomembranes*, *31*, 591–608.

Morgan, K., Stevens, E., Shah, B., Cox, P. J., Dixon, A. K., Lee, K., … Jackson, A. P. (2000). b3: An additional auxiliary subunit of the voltage-sensitive sodium channel that modulates channel gating with distinct kinetics. *Proceedings of the National Academy of Sciences of the USA*, *97*, 2308–2313.

Nakamura, N., Rabouille, C., Watsorusconin, R., Nilsson, T., Hui, N., Slusarewicz, P., … Warren, G. (1995). Characterization of a cis-Golgi matrix protein, GM130. *Journal of Cell Biology*, *131*, 1715–1726.

Orrico, A., Galli, L., Grosso, S., Buoni, S., Pianigiani, R., Balestri, P., & Sorrentino, V. (2009). Mutational analysis of the SCN1A, SCN1B and GABRG2 genes in 150 Italian patients with idiopathic childhood epilepsies. *Clinical Genetics*, *75*, 579–581.

Patino, G. A., Claes, L. R. F., Lopez-Santiago, L. F., Slat, E. A., Dondeti, R. S., Chen, C., … Isom, L. L. (2009). A functional null mutation of SCN1B in a patient with Dravet syndrome. *Journal of Neuroscience*, *29*, 10764–10778.

Patino, G. A., & Isom, L. L. (2010). Electrophysiology and beyond: Multiple roles of Na+ channel β subunits in development and disease. *Neuroscience Letters*, *486*, 53–59.

Ratcliffe, C. F., Westenbroek, R. E., Curtis, R., & Catterall, W. A. (2001). Sodium channel beta1 and beta3 subunits associate with neurofascin

through their extracellular immunoglobulin-like domain. *Journal of Cell Biology*, *154*, 427–434.

Rusconi, R., Combi, R., Cestèle, S., Grioni, D., Franceschetti, S., Dalprà, L., & Mantegazza, M. (2009). A rescuable folding defective Nav1.1 (SCN1A) sodium channel mutant causes GEFS+: Common mechanism in Nav1.1 related epilepsies? *Human Mutation*, *30*, E747–E760.

Rusconi, R., Scalmani, P., Cassulini, R. R., Giunti, G., Gambardella, A., Franceschetti, S., … Mantegazza, M. (2007). Modulatory proteins can rescue a trafficking defective epileptogenic Nav1.1 Na+ channel mutant. *Journal of Neuroscience*, *27*, 11037–11046.

Sampson, H. M., Thomas, D. Y., & Begley, T. P. (2007). Protein trafficking diseases: Small molecule approaches. *Wiley Encyclopedia of Chemical Biology*. https://doi.org/10.1002/9780470048672.wecb667

Schneider, C. A., Rasband, W. S., & Eliceiri, K. W. (2012). NIH Image to ImageJ: 25 years of image analysis. *Nature Methods*, *9*, 671–675.

Spampanato, J., Aradi, I., Soltesz, I., & Goldin, A. L. (2004). Increased neuronal firing in computer simulations of sodium channel mutations that cause generalized epilepsy with febrile seizures plus. *Journal of Neurophysiology*, *91*, 2040–2050.

Tammaro, P., Conti, F., & Moran, O. (2002). Modulation of sodium current in mammalian cells by an epilepsy-correlated β1-subunit mutation. *Biochemical and Biophysical Research Communications*, *291*, 1095–1101.

Thornhill, W. B., & Levinson, S. R. (1987). Biosynthesis of electroplax sodium channels in Electrophorus electrocytes and Xenopus oocytes. *Biochemistry*, *26*, 4381–4388.

Xu, R., Thomas, E. A., Gazina, E. V., Richards, K. L., Quick, M., Wallace, R. H., ... Petrou, S. (2007). Generalized epilepsy with febrile seizures plus-associated sodium channel beta1 subunit mutations severely reduce beta subunit-mediated modulation of sodium channel function. *Neuroscience*, *148*, 164–174.

Yu, F. H., & Catterall, W. A. (2003). Overview of the voltage-gated sodium channel family. *Genome Biology*, *4*, 207.

Yu, F. H., Westenbroek, R. E., Silos-Santiago, I., McCormick, K. A., Lawson, D., Ge, P., ... Curtis, R. (2003). Sodium channel beta4, a new disulfide-linked auxiliary subunit with similarity to beta2. *Journal of Neuroscience*, *23*, 7577–7585.

How to cite this article: Baroni D, Picco C, Moran O. A mutation of *SCN1B* associated with GEFS+ causes functional and maturation defects of the voltage-dependent sodium channel. *Human Mutation*. 2018;39:1402–1415. https://doi.org/10.1002/humu.23589